Electronic Supplementary Material (ESI) for New Journal of Chemistry.
This journal is © The Royal Society of Chemistry 2023

# Rapid and Scalable Synthesis of Sulfur Quantum Dots through Ozone Etching: Photoluminescence and FRET mediated $Co^{2+}$ Sensing

R V Reji,[a] V Biju*[a]

[a] Department of Physics, University of Kerala, Thiruvananthapuram- 695581, Kerala, India

**Table S1**. Comparison of different methods for the synthesis of luminescent SQDs from elemental sulfur.

| Synthetic method | Reaction time (h) | Reaction temperature (°C) | PLQY (%) | Reference |
|---|---|---|---|---|
| Assembly-fission synthesis | 125 | 70 | 3.8 | 1 |
| Assembly-fission followed by $H_2O_2$ etching | 125 | 70 | 23 | 2 |
| Hydrothermal fission-aggregation mechanism | 4 | 170 | 4.02 | 3 |
| Oxygen acceleration | 10 | 90 | 21.5 | 4 |
| Ultrasonication-promoted synthesis | 12 | - | 2.1 | 5 |
| Copper-Ion-Assisted Precipitation Etching Method | 74 | 70 | 32.8 | 6 |
| Microwave-assisted synthesis | 55 | 70 | 49.25 | 7 |
| Bubbling-assisted strategy | 96 | 70 | 8 | 8 |
| Ultrasound-microwave-assisted etching with hydrogen peroxide | 2 | 70 | 58.6 | 9 |
| Solvothermal Synthesis | 42 | 220 | 10.30 | 10 |
| Dielectric barrier discharge-accelerated one-pot synthesis | 20 | - | 2.0 | 11 |
| Mechanical grinding assisted approach | 1 | - | 21 | 12 |
| Ethylenediamine-assisted solvothermal treatment | 5 | 170 | 87.8 | 13 |
| Ethylenediamine-assisted acceleration strategy | 6 | 70 | 14.22 | 14 |
| Ethanol assisted solvothermal treatment | 36 | 220 | 7.04 | 15 |
| solvent-type passivation strategy | 4 | 160 | 8.7 | 16 |
| Ozone assisted top- down approach | 4 | 90 | 9.26 | Present work |

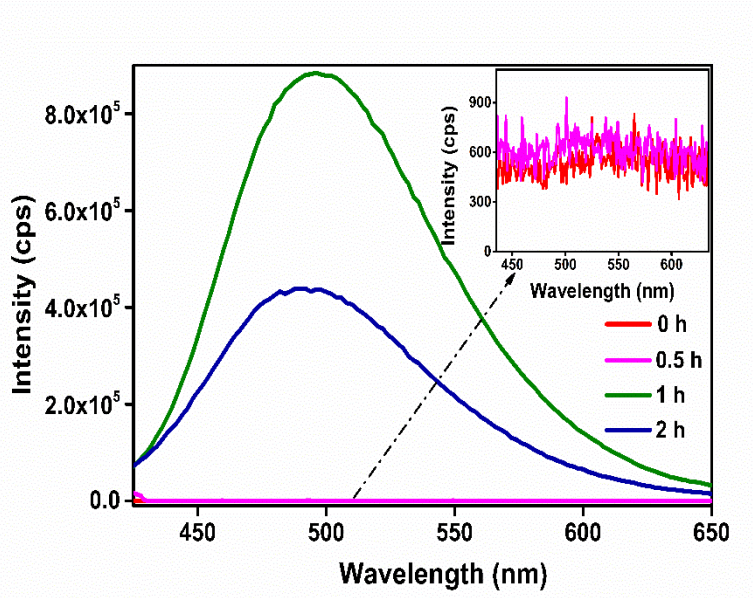


**Fig. S1**. PL spectra (excited at 410 nm) of S dots with different durations of ozone treatment as indicated on the frame.

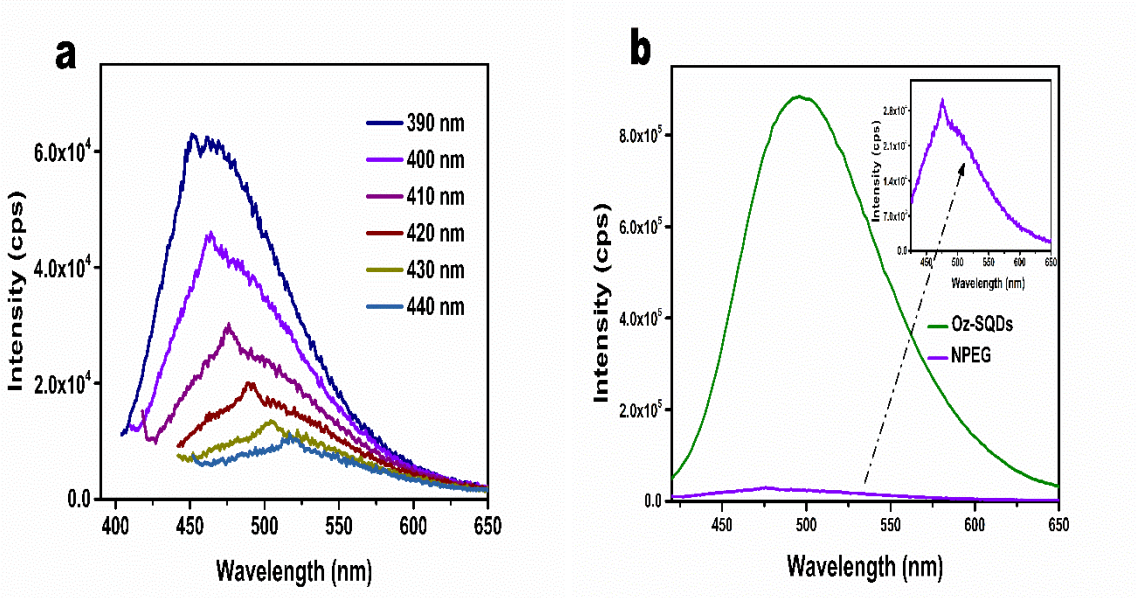


**Fig. S2**. (a) PL spectra of NPEG at different excitation wavelengths. (b) PL spectra (excited at 410 nm) of NPEG and Oz-SQDs.

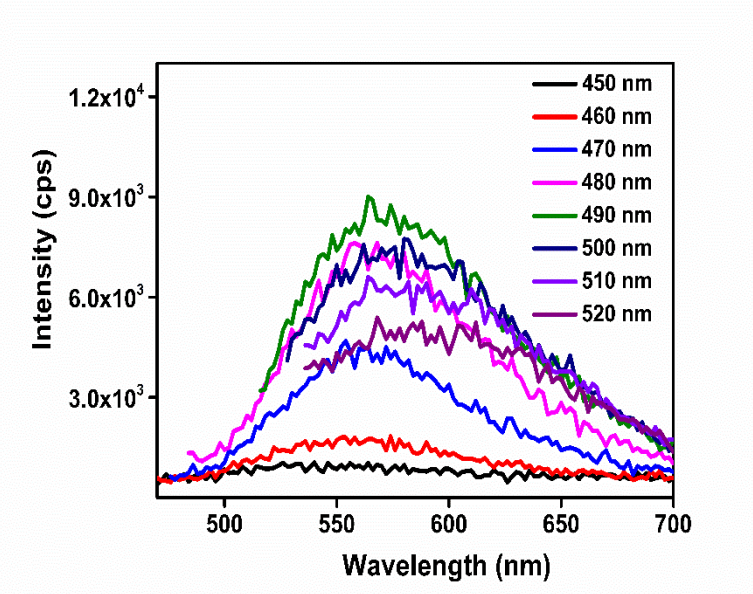


**Fig. S3**. Excitation-independent PL spectra of S dots.

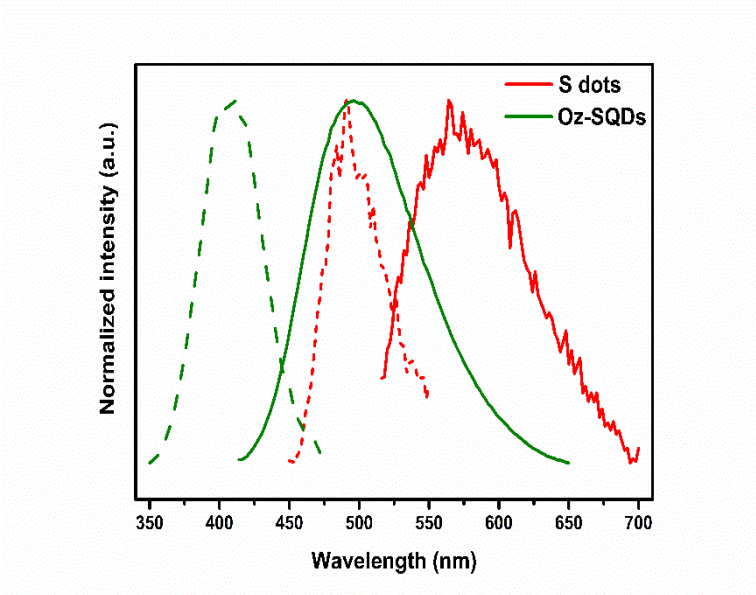


**Fig. S4.** PL (solid red line, excited at 490 nm), PLE (dash red line, detected at 575 nm) of S dots and PL (solid green line, excited at 410 nm), PLE (dash green line, detected at 496 nm) of Oz-SQDs.

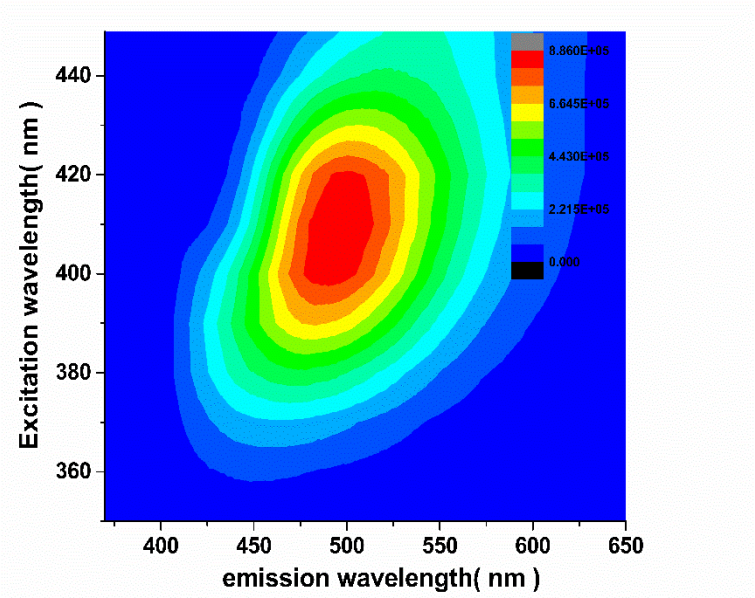


**Fig. S5**. The three-dimensional excitation and emission matrix (3D-EEM) fluorescence spectrum of Oz-SQDs.

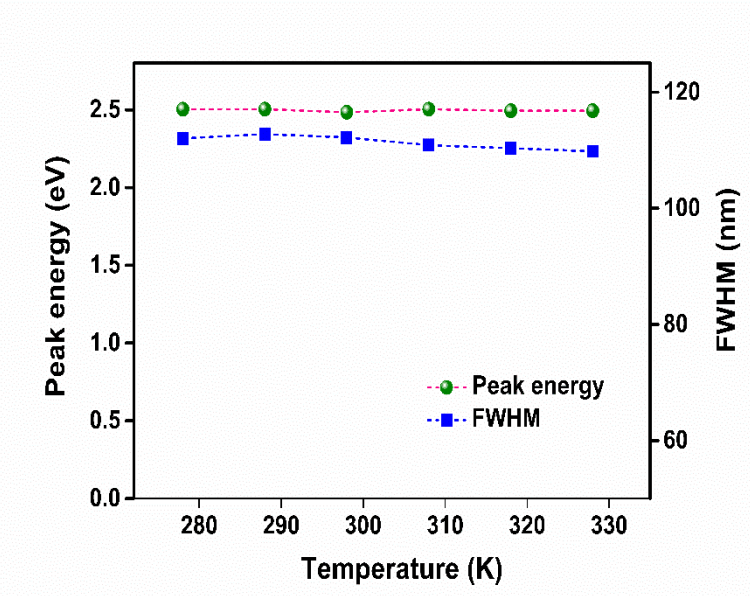


**Fig. S6**. PL peak energy and FWHM as a function of the temperature.

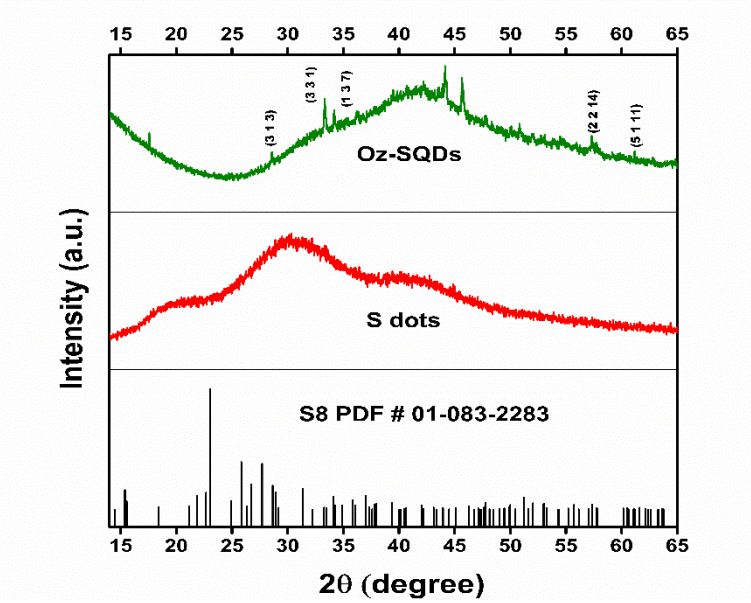


**Fig. S7**. XRD patterns of S dots and Oz- SQDs.

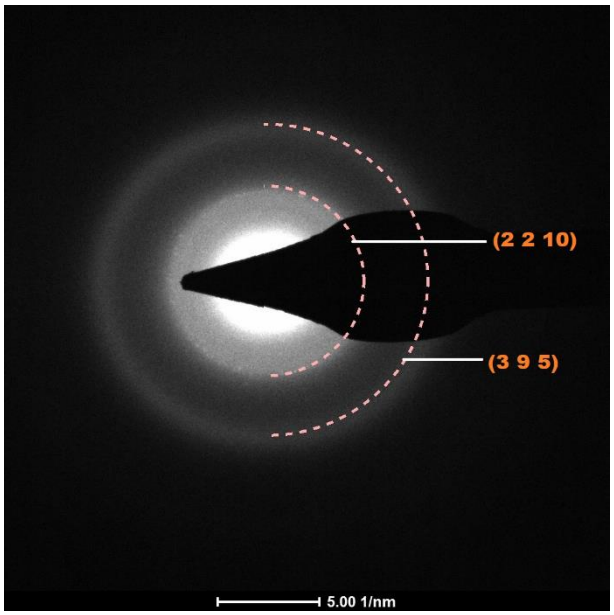


**Fig. S8**. SAED pattern of S dots.

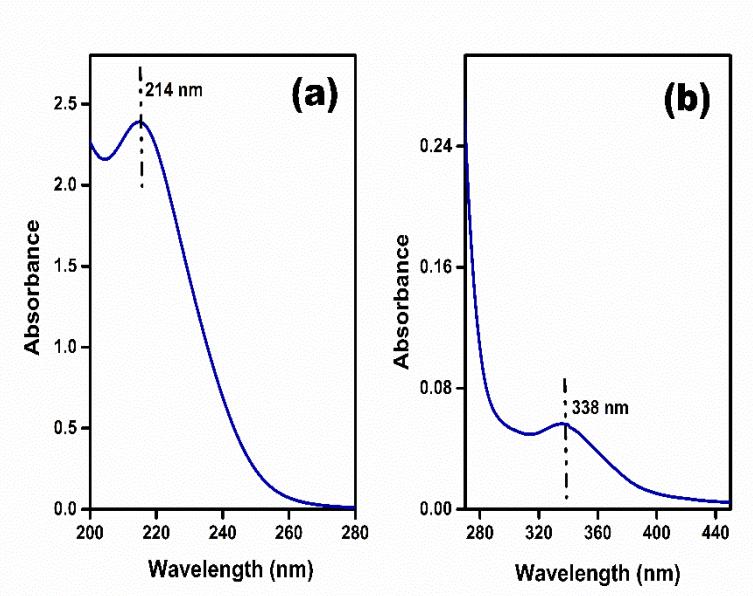


**Fig. S9.** UV-Visible absorption spectra of the sample with 2h ozone treatment after diluting (a) 2000 times with water (b) 100 times with water.

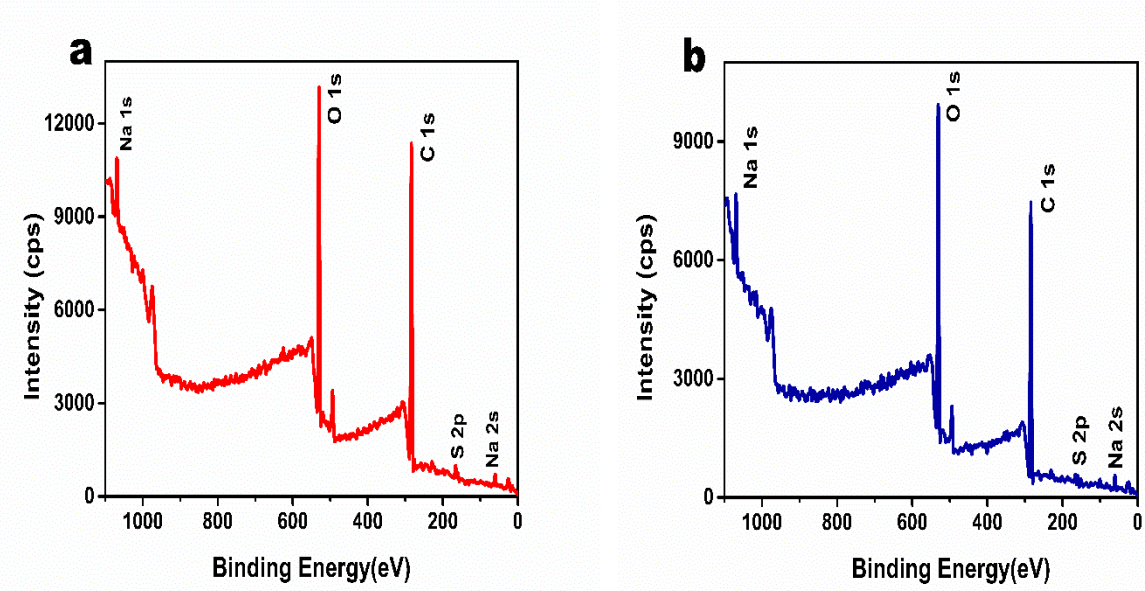


**Fig. S10.** (a) XPS survey spectra of (a) S dots (b) Sample with 2 h ozone treatment.

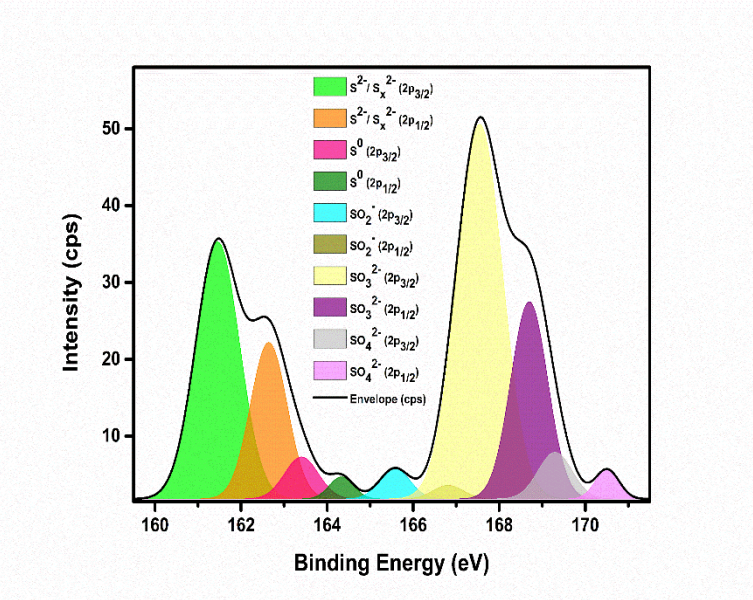


**Fig. S11.** S2p XPS spectrum of the sample with 2 h ozone treatment.

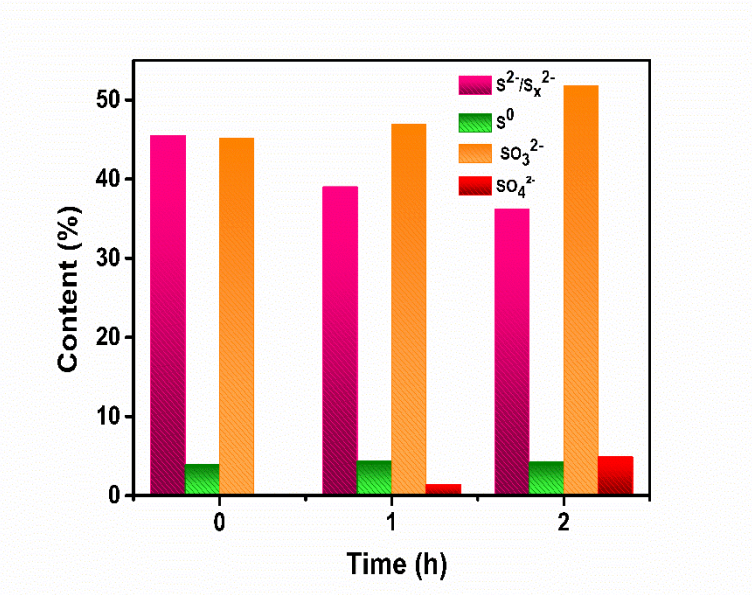


**Fig. S12.** Variation in the amount of different sulfur species with ozone treatment duration.

**Table S2**. Comparison of different methods for the determination of $Co^{2+}$.

| Methods | Sensing material | Linear range (µM) | Detection limit (µM) | Reference |
|---|---|---|---|---|
| Fluorometric | Carbon dots | 0 - 40 | 0.45 | [17] |
| Fluorometric | Nitrogen and sulfur co-doped graphene quantum dots | 0 - 40 | 1.25 | [18] |
| Potentiometric | p-(4-n-butylphenylazo) calix[4]arene | 9.2- 10000 | 4.00 | [19] |
| Colorimetric | Biofunctionalized silver nanoparticles | 5 - 100 | 7.00 | [20] |
| Fluorometric | Sulfur quantum dots | 0 - 90 | 0.02 | [21] |
| Fluorometric | Sulfur quantum dots | 0-25 | 1.57 | [22] |
| Fluorometric | Cysteine-decorated sulfur dots | 0 - 40 | 0.16 | [23] |
| Fluorometric | Sulfur quantum dots | 19.6 – 56.6 | 2.44 | Present work |

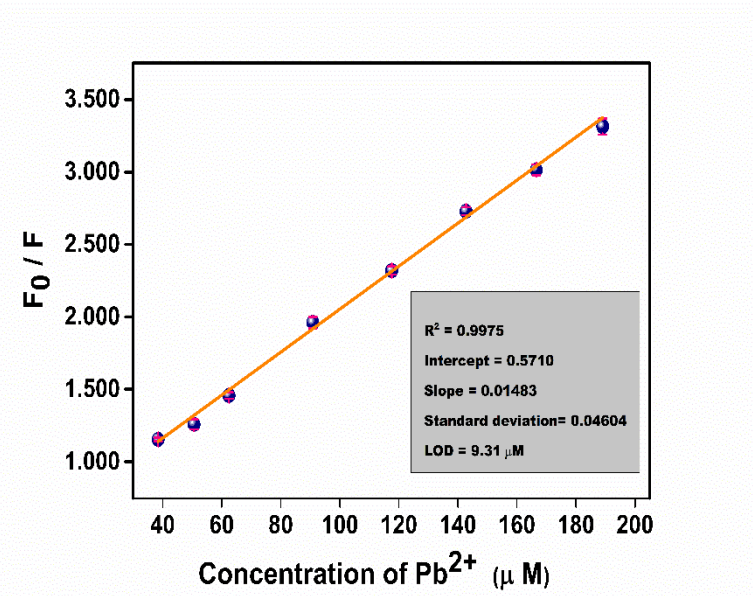


**Fig. S13.** $F_0$ /F value of the Oz-SQDs against different concentrations of $Pb^{2+}$.

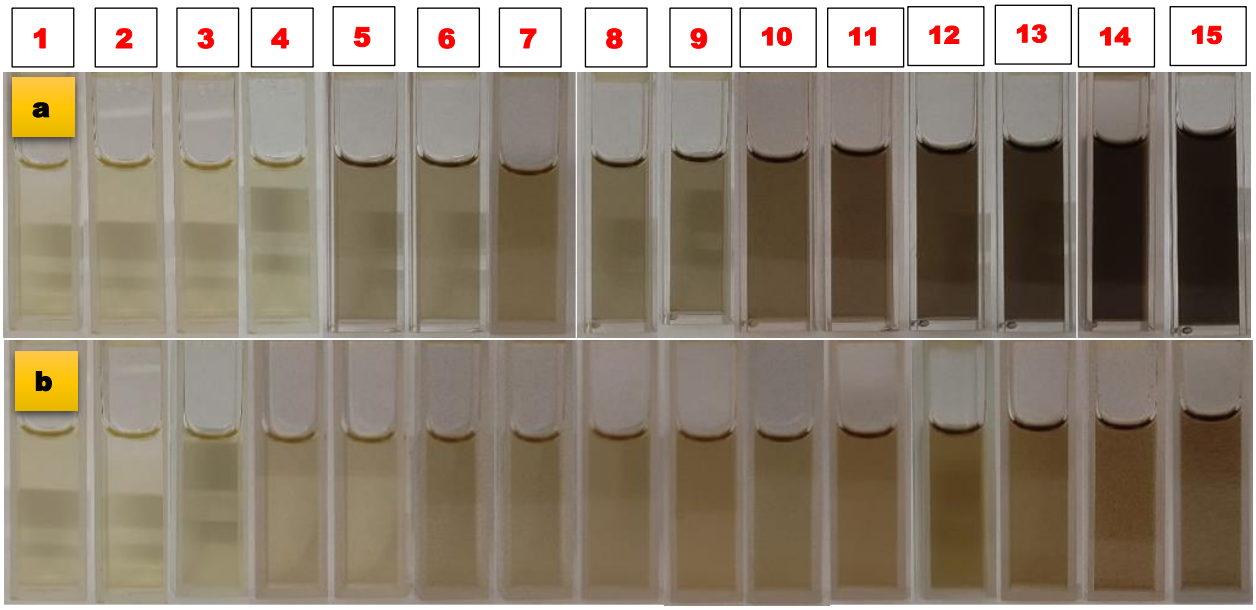


**Fig. S14.** Color of the Oz-SQDs aqueous solution after adding different concentrations of (a) $Co^{2+}$ (b) $Pb^{2+}$
[ (1). 0 µM, (2). 19.6 µM, (3). 22.8 µM, (4) 29.1 µM, (5) 32.2 µM, (6). 38.5 µM, (7). 44.6 µM (8) 56.6 µM, (9) 62.5 µM, (10). 90.9 µM, (11). 117.6 µM, (12). 142.8 µM, (13). 166.6 µM, (14). 210.5 µM, (15). 249.9 µM ]

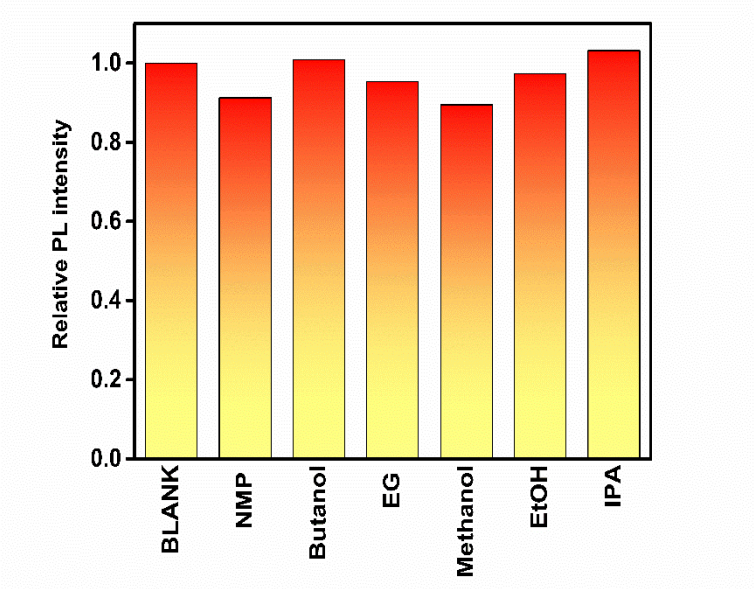


**Fig. S15.** Relative PL intensity of Oz-SQDs in the presence of different organic solvents (3 M); 1-Methyl-2-pyrrolidone (NMP), tert-Butanol ( Butanol), Ethylene glycol (EG), Methanol, Ethanol (EtOH), Isopropyl alcohol (IPA).

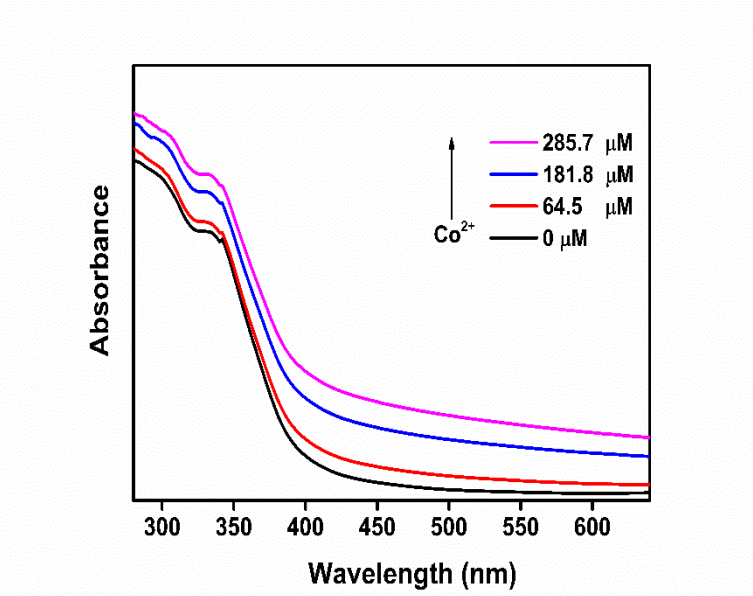


**Fig. S16.** UV-Visible absorption spectra of Oz-SQDs in the presence of different concentrations of $Co^{2+}$.

**Table S3.** PL lifetime components and corresponding amplitude fractions of Oz-SQDs and Oz-SQDs/ $Co^{2+}$ system.

| Sample | $\tau_1$ (ns) | $a_1$ (%) | $\tau_2$ (ns) | $a_2$ (%) | $\tau_{avg}$ (ns) |
|---|---|---|---|---|---|
| **Oz-SQDs** | **1.23** | **90.78** | **3.22** | **9.22** | **1.65** |
| **Oz-SQDs/ $Co^{2+}$** | **0.75** | **97.51** | **3.29** | **2.49** | **1.01** |

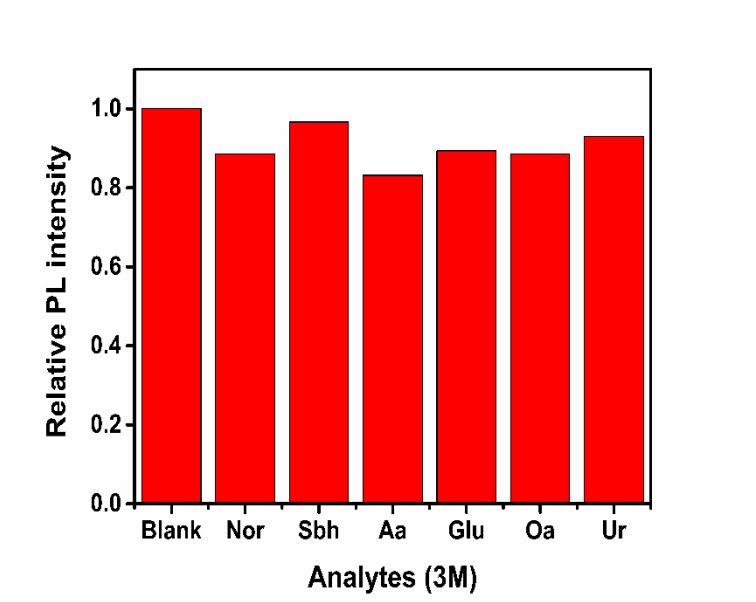


**Fig. S17.** Relative PL intensity of Oz-SQDs/ $Co^{2+}$ system in the presence of various reducing agents; Norfloxacin (Nor), Sodium borohydride (Sbh), Ascorbic acid (Aa), Glucose (Glu), Oxalic acid (Oa) and Urea (Ur).

## REFERENCES


1 L. Shen, H. Wang, S. Liu, Z. Bai, S. Zhang, X. Zhang and C. Zhang, *J. Am. Chem. Soc.*, 2018, **140**, 7878–7884.

2 H. Wang, Z. Wang, Y. Xiong, S. V. Kershaw, T. Li, Y. Wang, Y. Zhai and A. L. Rogach, *Angew. Chemie - Int. Ed.*, 2019, **58**, 7040–7044.

3 L. Xiao, Q. Du, Y. Huang, L. Wang, S. Cheng, Z. Wang, T. N. Wong, E. K. L. Yeow and H. Sun, *ACS Appl. Nano Mater.*, 2019, **2**, 6622–6628.

4 Y. Song, J. Tan, G. Wang, P. Gao, J. Lei and L. Zhou, *Chem. Sci.*, 2020, **11**, 772–777.

5 C. Zhang, P. Zhang, X. Ji, H. Wang, H. Kuang, W. Cao, M. Pan, Y. E. Shi and Z. Wang, *Chem. Commun.*, 2019, **55**, 13004–13007.

6 Q. Le Li, L. X. Shi, K. Du, Y. Qin, S. J. Qu, D. Q. Xia, Z. Zhou, Z. G. Huang and S. N. Ding, *ACS Omega*, 2020, **5**, 5407–5411.

7 Z. Hu, H. Dai, X. Wei, D. Su, C. Wei, Y. Chen, F. Xie, W. Zhang, R. Guo and S. Qu, *RSC Adv.*, 2020, **10**, 17266–17269.

8 S. Liu, H. Wang, A. Feng, J. Chang, C. Zhang, Y. Shi, Y. Zhai, V. Biju and Z. Wang, *Nanoscale Adv.*, 2021, **3**, 4271–4275.

9 Y. Sheng, Z. Huang, Q. Zhong, H. Deng, M. Lai, Y. Yang, W. Chen, X. Xia and H. Peng, *Nanoscale*, 2021, **13**, 2519–2526.

10 C. Wang, Z. Wei, C. Pan, Z. Pan, X. Wang, J. Liu, H. Wang, G. Huang, M. Wang and L. Mao, *Sensors Actuators, B Chem.*, 2021, **344**, 130326.

11 M. Yang, C. Li, Y. Tian, L. Wu, J. Hu and X. Hou, *Chem. Commun.*, 2022, **58**, 8614–8617.

12 K. S. Sunil, K. Bramhaiah, S. Mandal, S. Kar, N. S. John and S. Bhattacharyya, *Mater. Adv.*, 2022, **3**, 2037–2046.

13 P. Gao, Z. Huang, J. Tan, G. Lv and L. Zhou, *ACS Sustainable. Chem. Eng.*, 2022, **10**, 4634–4641.

14 F. Yan, M. Xu, J. Xu, Y. Wang, C. Yi, Y. Dong, X. Wang and J. Xu, *Sensors Actuators B Chem.*, 2022, **370**, 132393.

15 Z. Wei, W. Lu, C. Pan, J. Ni, H. Zhao, G. Huang and C. Wang, *Dalt. Trans.*, 2022, **51**, 10290–10297.

16 C. Wu, S. Zhang, Y. Zheng, A. Wang, Q. Zhao, W. Sun, W. Liu, C. Long and Q. Wang, *Inorg. Chem.*, 2022, **61**, 21157–21168.

17 D. Kong, F. Yan, Z. Han, J. Xu, X. Guo and L. Chen, *RSC Adv.*, 2016, **6**, 67481–67487.

18 W. Boonta, C. Talodthaisong, S. Sattayaporn, C. Chaicham, A. Chaicham, S. Sahasithiwat, L. Kangkaew and S. Kulchat, *Mater. Chem. Front.*, 2020, **4**, 507–516.

19 P. Kumar and Y. B. Shim, *Talanta*, 2009, **77**, 1057–1062.

20 Y. Yao, D. Tian and H. Li, *ACS Appl. Mater. Interfaces*, 2010, **2**, 684–690.

21 S. Wang, X. Bao, B. Gao and M. Li, *Dalt. Trans.*, 2019, **48**, 8288–8296.

22 F. Arshad and M. P. Sk, *ACS Appl. Nano Mater.*, 2020, **3**, 3044–3049.

23 L. Li, C. Yang, Y. Li, Y. Nie and X. Tian, *J. Mater. Sci.*, 2021, **56**, 4782–4796.